STEM CELLS AND DEVELOPMENT
Volume 22, Number 18, 2013

DOI: 10.1089/scd.2012.0623

Ddx46 Is Required for Multi-Lineage Differentiation of Hematopoietic Stem Cells in Zebrafish

Ryo Hirabayashi,[1,*] Shunya Hozumi,[1,*] Shin-ichi Higashijima,[2,3] and Yutaka Kikuchi[1]

Balanced and precisely controlled processes between self-renewal and differentiation of hematopoietic stem cells (HSCs) into all blood lineages are critical for vertebrate definitive hematopoiesis. However, the molecular mechanisms underlying the maintenance and differentiation of HSCs have not been fully elucidated. Here, we show that zebrafish *Ddx46*, encoding a DEAD-box RNA helicase, is expressed in HSCs of the caudal hematopoietic tissue (CHT). The number of HSCs expressing the molecular markers *cmyb* or T-cell acute lymphocytic leukemia 1 (*tal1*) was markedly reduced in *Ddx46* mutants. However, massive cell death of HSCs was not detected, and proliferation of HSCs was normal in the CHT of the mutants at 48 h postfertilization. We found that myelopoiesis occurred, but erythropoiesis and lymphopoiesis were suppressed, in *Ddx46* mutants. Consistent with these results, the expression of *spi1*, encoding a regulator of myeloid development, was maintained, but the expression of *gata1a*, encoding a regulator of erythrocyte development, was downregulated in the mutants. Taken together, our results provide the first genetic evidence that zebrafish Ddx46 is required for the multilineage differentiation of HSCs during development, through the regulation of specific gene expressions.

Introduction

It has been well noted that the processes involved in vertebrate hematopoiesis during development consist of two evolutionarily conserved steps: primitive hematopoiesis followed by definitive blood formation [1–3]. In the definitive hematopoiesis stage, all blood lineages arise from self-renewing hematopoietic stem cells (HSCs), and hematopoiesis derived from HSCs persists for the lifetime of vertebrates [1–3]. In recent years, zebrafish has been used as an excellent vertebrate system for studying hematopoiesis during development [4,5]. In the definitive hematopoietic wave of zebrafish embryos, HSCs originate from the ventral wall of the dorsal aorta (VDA) in the aorta-gonad-mesonephros (AGM) region [2–4]. These HSCs then migrate to an intermediate hematopoietic site, the caudal hematopoietic tissue (CHT), and then further toward the kidney or the thymus, which are definitive hematopoietic or lymphopoietic organs, respectively, in adult zebrafish [2–4].

Several lines of genetic evidence have revealed that at least two transcription factors, cMyb and Runt-related transcription factor 1 (Runx1), have been implicated in the initiation, maintenance, and/or differentiation of HSCs during vertebrate development [5–14]. Studies on murine and human hematopoietic cell lines have shown that the *cmyb* proto-oncogene, encoding a transcription factor, is expressed mainly in HSCs, and its expression is downregulated in differentiated hematopoietic cells [5]. In addition, studies in a mouse model have suggested that cMyb plays critical roles in HSC maintenance and differentiation during development [6–8]. Consistent with observations that have been made in mice, zebrafish *cmyb* mutants have defects in definitive hematopoiesis, suggesting that cMyb function is evolutionarily conserved [9,10]. On the other hand, *runx1* is expressed in the VDA of mouse and zebrafish embryos [11,12], and analyses of Runx1 knockout mice and zebrafish mutants have revealed that Runx1 is required for the emergence of HSCs at the beginning of definitive hematopoiesis [5,13,14]. In contrast to these 2 factors, analyses of mutant animals have shown that the T-cell acute lymphocytic leukemia 1 (*Tal1*; also known as *Scl*) gene, encoding a basic-helix-loop-helix transcription factor, is required for both hematopoietic and endothelial development [1,2,5]. Further, in vitro experiments using mouse embryonic stem cells revealed that Tal1 plays critical roles in both hemogenic endothelium population generation and definitive hematopoietic specification [15]. Further, the function of Tal1 is upstream of Runx1 in definitive hematopoiesis [15]. The molecular mechanisms

[1]Department of Biological Science, Graduate School of Science, Hiroshima University, Hiroshima, Japan.
[2]National Institutes of Natural Sciences, Okazaki Institute for Integrative Bioscience, National Institute for Physiological Sciences, Okazaki, Aichi, Japan.
[3]Graduate University for Advanced Studies, Okazaki, Aichi, Japan.
*These two authors contributed equally to this work.

underlying the initiation, maintenance, and differentiation of HSCs, however, remain to be elucidated.

DExD/H-box proteins belong to an evolutionarily conserved family of RNA helicases [16,17]. The DExD/H-box RNA helicases are known to function in all aspects of RNA metabolism such as pre-mRNA splicing, rRNA biogenesis, and transcription by using the energy derived from ATP hydrolysis [16,17]. By genetic screening using zebrafish, two DExD/H-box genes, *Ddx18* and *Dhx8*, have been identified thus far as novel genes that are essential for hematopoiesis [18,19]. A recent study has reported that Ddx18 is required for primitive hematopoiesis through the regulation of p53-dependent G1 cell-cycle arrest [18]. Moreover, a sequence variation in human DDX18, which acts as a dominant-negative, was identified in samples from patients with acute myeloid leukemia [18]. A more recent report showed that a mutation in Dhx8, a zebrafish orthologue of the yeast splicing factor Prp22, led to defects in cell division, pre-mRNA splicing, and primitive hematopoiesis [19]. However, the requirement and function of the DExD/H-box RNA helicases in hematopoiesis are still largely unknown in vertebrates.

Our previous study has shown that Ddx46, a member of the DEAD-box RNA helicase family, is required for the development of digestive organs and the brain, possibly by regulating pre-mRNA splicing [20]. Here, we show zebrafish *Ddx46* expression in HSCs during development. Moreover, we investigated the phenotype of a zebrafish *Ddx46* mutant in definitive hematopoiesis, and we report the function of Ddx46 in HSC differentiation during development.

Materials and Methods

Ethics statement

All animal experiments were conducted according to relevant national and international guidelines "Act on Welfare and Management of Animals" (Ministry of Environment of Japan). Ethics approval from the Hiroshima University Animal Research Committee (HuARC) was not sought since this law does not mandate protection of fish.

Maintenance and staging of zebrafish

Adult zebrafish and zebrafish embryos were maintained as described by Westerfield [21]. Embryos were incubated in 1/3 Ringer's solution (39 mM NaCl, 0.97 mM KCl, 1.8 mM $CaCl_2$, and 1.7 mM HEPES, pH 7.2) at 28.5°C and staging was performed as described by Kimmel et al. [22]. The *Ddx46* allele *hi2137* was isolated during an insertional mutagenesis screening (http://web.mit.edu/hopkins/group11.html) [23], and the $Ddx46^{hi2137/+}$ fish was obtained from the Zebrafish International Resource Center.

Generation of Tg(tal1:EGFP) fish

Approximately 8 kb of the 5′ upstream sequence of *tal1* [24,25] was polymerase chain reaction (PCR)-amplified from zebrafish genomic DNA. The amplified *tal1* promoter, *EGFP*, and *SV40 poly(A)* were placed in the pT2KXIGΔin vector that has *Tol2* transposable elements [26]. Microinjection of *Tol2*-based plasmid DNA was performed as described previously [26].

Whole-mount in situ hybridization, immunohistochemistry, detection of cell death, and genotyping

Single and double whole-mount in situ hybridizations were performed as described previously [21,27], and riboprobes were prepared according to previously published methods. To detect apoptotic cells, we performed TUNEL staining using an in situ Cell Death Detection Kit (Roche Diagnostics) according to the manufacturer's instructions. In addition to TUNEL staining, we performed acridine orange staining for apoptosis detection. Live larvae were stained with 10 μg/mL of acridine orange [acridine orange hemi (zinc chloride) salt; Sigma] in 1/3 Ringer's solution for 15 min, and then washed thrice with 1/3 Ringer's solution for 5 min each. To evaluate cell proliferation, we performed whole-mount immunohistochemistry as described previously [21]. Mouse monoclonal anti-proliferating cell nuclear antigen (PCNA) antibody (Sigma) and Alexa Fluor® 594 goat anti-mouse IgG antibody (Invitrogen, Life Technologies Corp.) were used as primary and secondary antibodies, respectively. The stained embryos/larvae were embedded in 0.5% low melting temperature agarose in 1/3 Ringer's solution and imaged on an Olympus FV1000-D confocal microscope. Following the whole-mount in situ hybridization, TUNEL staining, or immunohistochemical staining, $Ddx46^{hi2137/hi2137}$ mutants were confirmed by genotyping as described previously [20].

mRNA and DNA injections

The pCS2+ vector carrying a cDNA fragment encoding *Ddx46*, *EGFP*, or *Tol2*-transposase [26] was used in this study. Capped mRNA was synthesized using an SP6 mMESSAGE mMACHINE (Ambion, Life Technologies Corp.). For the overexpression experiments, *Ddx46* or *EGFP* mRNA (320 pg each) was injected at the one-cell stage.

For phenotypic rescue experiments of *GATA*-binding protein 1a (*gata1a*) [28], *Tol2*-mediated transgenesis was performed as described previously [29]. At the one-cell stage, 12.5 pg of pT8.1gata1Δ 3-EGFP (pT-EGFP), which contained the promoter region of *gata1a* and *EGFP*, or pT8.1gata1Δ 3-FLgata1 (pT-FLgata1), which contained the promoter region of *gata1a* and FLAG-tagged *gata1a*, was co-injected with 25 pg of *Tol2*-transposase mRNA [29].

Quantitative real-time PCR

Total RNA was prepared using TRIzol (Invitrogen, Life Technologies Corp.) from the tails of 50 combined samples of the 3 days postfertilization (dpf) control (con) or $Ddx46^{hi2137/hi2137}$ mutant larvae that were identified morphologically or molecularly. Con larvae were sibling wild-type (WT) or $Ddx46^{hi2137/+}$ larvae, and they had normal phenotypes. DNase-treated RNA (750 ng) was reverse transcribed with random 9-mer priming and reverse transcriptase XL (AMV) (TaKaRa). Quantitative PCR (qPCR) for *spi1* (also known as *pu.1*) [30] and *gata1a* was performed in triplicate using the Thermal Cycler Dice® Real Time System, SYBR® *Premix Ex Taq*™ (TaKaRa Bio, Inc.), and total RNA prepared as described above, according to the manufacturer's instructions. The amplified signals were confirmed to be a single band by gel electrophoresis, and they were normalized to the signals of zebrafish 18S rRNA. The primers used were as follows: *gata1a*, 5′-GGCTAGTTCACTCCATGATC-3′ and 5′-CTCAG

AGCTGGAGTAGAAAG-3′; *spi1*, 5′-ATGTGGAGTCCAGCC ATTTC-3′ and 5′-TTGTGAGGGTAACACACCGA-3′; 18S rRNA, 5′-CCGCTAGAGGTGAAATTCTTG-3′ and 5′-CAG CTTTGCAACCATACTCC-3′.

Reverse transcription-PCR analysis of splicing

Reverse transcription (RT)-PCR was performed using total RNA prepared as described above to monitor the splicing of *spi1*, *gata1a*, and *cmyb*. The primer pairs and detailed PCR conditions used to amplify each of these genes are listed in the Supplementary Tables S1 and S2 (Supplementary Data are available online at www.liebertpub.com/scd).

Results

Ddx46$^{hi2137/hi2137}$ mutants have defects in definitive hematopoiesis but not primitive hematopoiesis

We have previously shown that *Ddx46$^{hi2137/hi2137}$* mutants have defects in the formation of digestive organs and the brain [20]. In the course of the phenotypic analyses of *Ddx46$^{hi2137/hi2137}$* mutants, we also found that the expression of hematopoietic markers was downregulated in the mutants. At 22 hours postfertilization (hpf), the expression of the primitive hematopoietic markers *tal1*, *LIM* domain only 2 (*lmo2*) [31], *gata1a*, hemoglobin beta embryonic-3 (*hbbe3*) [32], and myeloid-specific peroxidase (*mpx*) [33] was normal in *Ddx46$^{hi2137/hi2137}$* mutants (Fig. 1A–J). On the other hand, the expression of the HSC markers *tal1*, *runx1*, and *cmyb* was markedly reduced in *Ddx46$^{hi2137/hi2137}$* mutants at 3 dpf (Fig. 1K–P). These results indicate that definitive hematopoiesis, but not primitive hematopoiesis, was defective in the mutants.

To confirm that the loss of *Ddx46* is responsible for the observed phenotype in definitive hematopoiesis, we compared the expression pattern of *Ddx46* with that of *cmyb* in the CHT. Ubiquitous expression of *Ddx46* in the AGM and CHT was observed at 2 dpf (Fig. 2A), and dotted expression of *Ddx46* was found in the CHT at 3 dpf (Fig. 2B, C). At 4 dpf, the dotted expression pattern of *Ddx46* in the CHT was similar to the expression pattern of *cmyb* (Fig. 2D, E). Moreover, the expression of both genes overlapped in the CHT, as analyzed by double whole-mount in situ staining (Fig. 2F), indicating that *Ddx46* is expressed in the HSCs at 4 dpf. We next examined whether rescue was achieved by the overexpression of *Ddx46* mRNA. The expressions of *cmyb* and *tal1* were rescued in the *Ddx46* mRNA-injected *Ddx46$^{hi2137/hi2137}$* mutants (*cmyb*, 19 of 21 *Ddx46* mRNA-injected mutants were rescued; *tal1*, 19 of 22 *Ddx46* mRNA-injected mutants were rescued; Fig. 3C, F), compared with that in the *EGFP* mRNA-injected *Ddx46$^{hi2137/hi2137}$* mutants (*cmyb*, 0 of 26 *EGFP* mRNA-injected mutants were rescued; *tal1*, 0 of 21 *EGFP* mRNA-injected mutants were rescued; Fig. 3B, E) at 3 dpf. The overlapping expression of *Ddx46* and *cmyb* in the CHT and data from the rescue experiments clearly indicate that the defects in definitive hematopoiesis in *Ddx46$^{hi2137/hi2137}$* mutants are caused by the loss of *Ddx46*.

Expression of molecular markers for HSCs decreases in Ddx46$^{hi2137/hi2137}$ mutants without cell death or cell growth defects

Previous studies on zebrafish and mouse development showed that HSCs originate from the VDA in the AGM, and

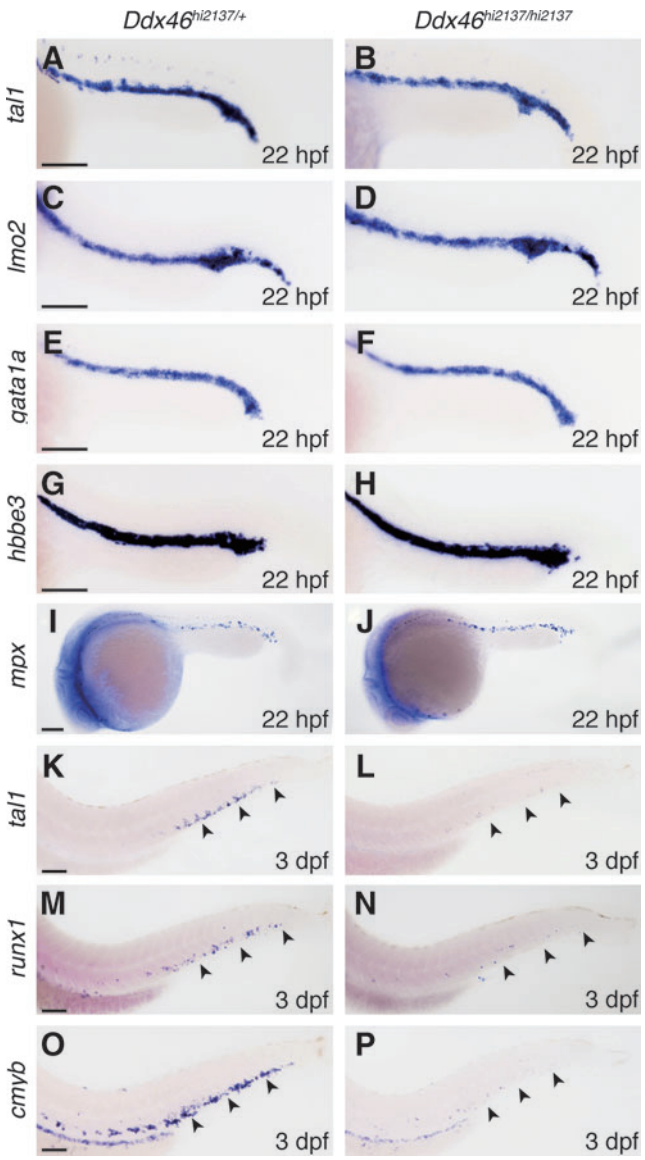

FIG. 1. Definitive, but not primitive, hematopoiesis is defective in *Ddx46$^{hi2137/hi2137}$* mutants. **(A–J)** The expression of primitive hematopoietic markers, *tal1*, *lmo2*, *gata1a*, *hbbe3*, and *mpx*, and definitive hematopoietic markers, *tal1*, *runx1*, and *cmyb* was examined by whole-mount in situ hybridization at 22 hpf and 3 dpf, respectively. All are lateral views, anterior to the *left*. The expression of *tal1*, *lmo2*, *gata1a*, *hbbe3*, and *mpx* was indistinguishable between *Ddx46$^{hi2137/+}$* (*tal1*, $n=9/9$; *lmo2*, $n=11/11$; *gata1a*, $n=9/9$; *hbbe3*, $n=12/12$; *mpx*, $n=16/16$) and *Ddx46$^{hi2137/hi2137}$* embryos (*tal1*, $n=9/9$; *lmo2*, $n=9/9$; *gata1a*, $n=7/7$; *hbbe3*, $n=10/10$; *mpx*, $n=7/7$) at 22 hpf **(A–J)**. In contrast, the number of cells expressing *tal1*, *runx1*, and *cmyb* in *Ddx46$^{hi2137/hi2137}$* larvae (*tal1*, $n=6/6$; *runx1*, $n=9/9$; *cmyb*, $n=11/11$) was markedly reduced compared with that in *Ddx46$^{hi2137/+}$* larvae (*tal1*, $n=8/8$; *runx1*, $n=11/11$; *cmyb*, $n=13/13$) at 3 dpf **(***arrowheads* in **K–P)**. Scale bars represent 100 μm. *tal1*, T-cell acute lymphocytic leukemia 1; hpf, hours postfertilization; *lmo2*, *LIM* domain only 2; *hbbe3*, hemoglobin beta embryonic-3; *mpx*, myeloid-specific peroxidase; dpf, days postfertilization. Color images available online at www.liebertpub.com/scd

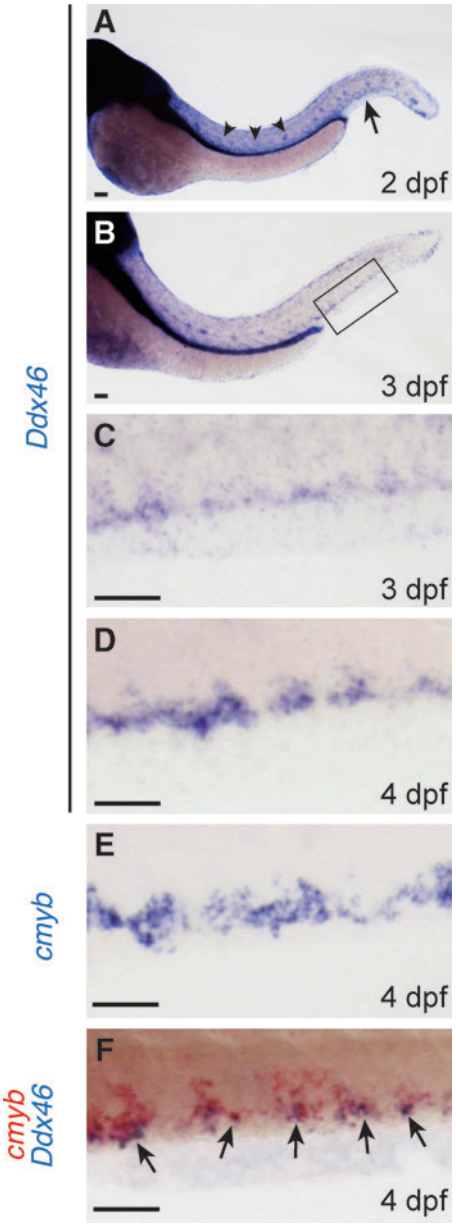

FIG. 2. *Ddx46* expression in HSCs. The expression of *Ddx46* and *cmyb* in wild-type larvae was examined by whole-mount in situ hybridization at 2, 3, and 4 dpf. All are lateral views, anterior to the *left*. **(A-C)** *Ddx46* is ubiquitously expressed in the AGM (*arrowheads* in **A)** and CHT (*arrow* in **A)** at 2 dpf ($n=6/6$) and is specifically expressed in the CHT (*boxed area* in **B)** at 3 dpf ($n=6/6$). The *boxed area* in **(B)** is shown enlarged in **(C)**. **(D, E)** The transcripts of both genes (*Ddx46*, $n=11/11$; *cmyb*, $n=9/9$) were detected in the CHT at 4 dpf. **(F)** Double whole-mount in situ staining showed that the expression domains of *Ddx46* (*blue*) and *cmyb* (*red*) overlapped in the CHT (*arrows*) ($n=7/7$) at 4 dpf. Scale bars represent 50 μm. HSCs, hematopoietic stem cells; AGM, aorta-gonad-mesonephros; CHT, caudal hematopoietic tissue. Color images available online at www.liebertpub.com/scd

they then migrate to the CHT [2–4]. To determine when definitive hematopoiesis was affected in *Ddx46*$^{hi2137/hi2137}$ larvae, we next counted the number of *cmyb*-expressing HSCs at 36 hpf, 48 hpf, and 3 dpf. The number of *cmyb*-expressing HSCs was indistinguishable between *Ddx46*$^{hi2137/+}$ (Fig. 4A, G) and *Ddx46*$^{hi2137/hi2137}$ larvae (Fig. 4B, G) at 36 hpf. In contast, the number of *cmyb*-expressing HSCs in the CHT, but not in the AGM, at 48 hpf and in both the AGM and CHT at 3 dpf was lower in *Ddx46*$^{hi2137/hi2137}$ larvae (Fig. 4D, F, G) than in *Ddx46*$^{hi2137/+}$ larvae (Fig. 4C, E, G). To exclude the possibility that the formation of the VDA is affected in *Ddx46*$^{hi2137/hi2137}$ mutants, we examined the expressions of *runx1* and kinase insert domain receptor like (*kdrl*; also known as *flk1*) [31], an endothelial marker, in the VDA at 48 hpf. The expression of these genes was normal in the mutants at this stage (Supplementary Fig. S1). These results suggest that the emergence of HSCs from the VDA is normal, but the expression of *cmyb*, a molecular marker for HSCs is not maintained in *Ddx46*$^{hi2137/hi2137}$ mutants.

Possible explanations for the reduction of *tal1*-, *runx1*-, or *cmyb*-expressing HSCs in *Ddx46*$^{hi2137/hi2137}$ larvae are the upregulation of cell death or the downregulation of cell proliferation. We first examined cell death of HSCs in the AGM and CHT from 36 hpf to 4 dpf by TUNEL analysis and acridine orange staining because massive apoptosis was observed in digestive organs and the brain of *Ddx46*$^{hi2137/hi2137}$ larvae at 3 dpf, and these larvae cannot survive beyond 5 dpf [20]. From 24 hpf to 4 dpf, increased cell death was not detected in the AGM or CHT of the *Ddx46*$^{hi2137/hi2137}$ larvae (Fig. 5 and Supplementary Fig. S2, and data not shown) compared with that in the *Ddx46*$^{hi2137/+}$ larvae. We next examined cell proliferation using the *Ddx46*^{hi2137}; Tg(*tal1:EGFP*) transgenic line. Confocal images of the anti-PCNA immunostaining and EGFP fluorescence indicated that the proliferation of *tal1*-expressing HSCs was indistinguishable between *Ddx46*$^{hi2137/+}$ and *Ddx46*$^{hi2137/hi2137}$ larvae at 48 hpf (Fig. 6). It was very difficult to estimate cell proliferation of HSCs after 2.5 dpf because the EGFP fluorescence and the number of EGFP^{+} cells were profoundly reduced in *Ddx46*$^{hi2137/hi2137}$ larvae at these stages (Supplementary Fig. S3). These results indicate that the reduction of *tal1*-expressing HSCs in *Ddx46*$^{hi2137/hi2137}$ larvae is not caused by the upregulation of cell death in the AGM and CHT or by the downregulation of cell proliferation of HSCs at 48 hpf.

Myelopoiesis occurs, but erythropoiesis and lymphopoiesis are suppressed in the CHT of Ddx46$^{hi2137/hi2137}$ *mutants*

An alternative possibility for the reduction of HSCs in *Ddx46*$^{hi2137/hi2137}$ larvae is that the multipotency of HSCs may be lost, and premature differentiation of HSCs to blood lineages may occur in *Ddx46*$^{hi2137/hi2137}$ mutants. To test this hypothesis, we examined the expression of various molecular markers for definitive hematopoiesis by whole-mount in situ hybridization. The expression of an erythroid marker hemoglobin alpha embryonic-1 (*hbae1*) [32] was markedly reduced in *Ddx46*$^{hi2137/hi2137}$ mutants at 3 dpf (Fig. 7A, B). We further found that the expression of lymphoid makers, IKAROS family zinc finger 1 (*ikzf1*) [34] and recombination activating gene 1 (*rag1*) [35], was lost in the thymus of *Ddx46*$^{hi2137/hi2137}$ mutants at 4 dpf (Fig. 7C–F). However, the expression of forkhead box N1 (*foxn1*) [36], a thymus epithelial marker, was indistinguishable between *Ddx46*$^{hi2137/+}$ and *Ddx46*$^{hi2137/hi2137}$ larvae (Fig. 7G, H), indicating that thymus formation is normal in these mutants. Next, we tested the expression of myeloid markers such as lymphocyte cytosolic

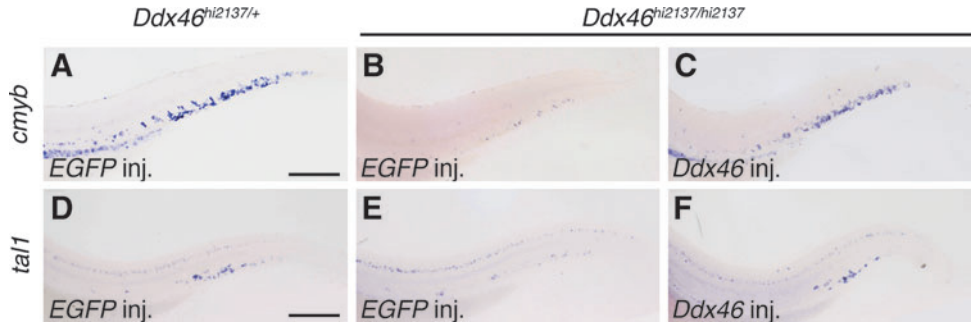

FIG. 3. Expression of *cmyb* and *tal1* in *Ddx46*$^{hi2137/hi2137}$ mutants is rescued by overexpression of *Ddx46* mRNA. **(A–F)** The expression of *cmyb* and *tal1* was examined by whole-mount in situ hybridization at 3 dpf. All are lateral views, anterior to the *left*. The number of *cmyb*- or *tal1*-expressing HSCs in the *EGFP* mRNA-injected *Ddx46*$^{hi2137/hi2137}$ larvae (*cmyb*, 0 of 26 *EGFP* mRNA-injected mutants were rescued; *tal1*, 0 of 21 *EGFP* mRNA-injected mutants were rescued) was markedly lower than that in the *EGFP* mRNA-injected *Ddx46*$^{hi2137/+}$ larvae (*cmyb*, $n=17/17$; *tal1*, $n=16/16$) at 3 dpf **(A, B, D, E)**. The overexpression of *Ddx46* mRNA was able to rescue the number of *cmyb*- or *tal1*-expressing HSCs in *Ddx46*$^{hi2137/hi2137}$ larvae (*cmyb*, 19 of 21 *Ddx46* mRNA-injected mutants were rescued; *tal1*, 19 of 22 *Ddx46* mRNA-injected mutants were rescued) at 3 dpf **(B, C, E, F)**. Scale bars represent 100 μm. Color images available online at www.liebertpub.com/scd

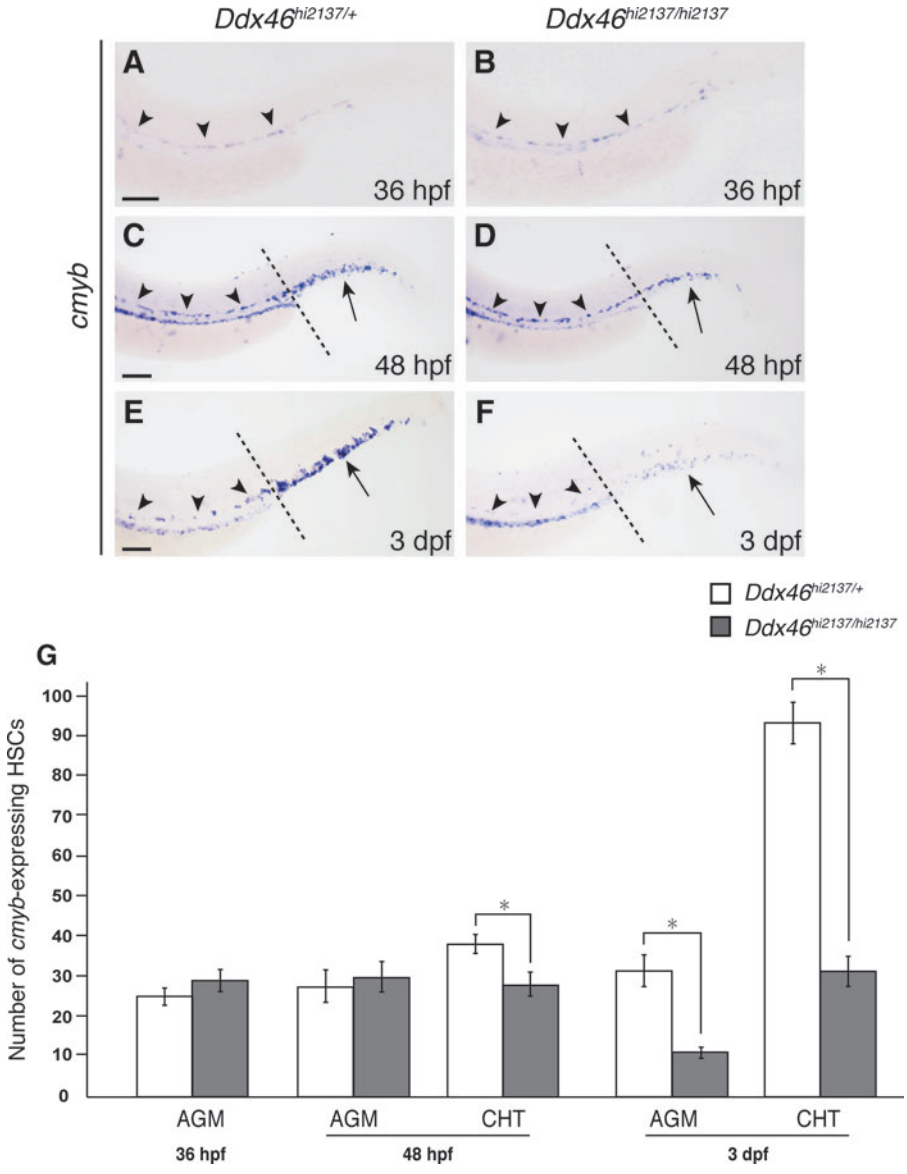

FIG. 4. Number of *cmyb*-expressing cells decreases in *Ddx46*$^{hi2137/hi2137}$ mutants. **(A–G)** The expression of *cmyb* was examined by whole-mount in situ hybridization at 36 hpf, 48 hpf, or 3 dpf. All are lateral views, anterior to the *left*. The number of *cmyb*-expressing HSCs in the AGM (*arrowheads*) and CHT (*arrows*) was counted at 36 hpf, 48 hpf, and 3 dpf **(G)**. At 36 hpf, the number of *cmyb*-expressing HSCs in the AGM (*arrowheads*) was indistinguishable between *Ddx46*$^{hi2137/+}$ and *Ddx46*$^{hi2137/hi2137}$ larvae **(A, B, G)**. In contrast, the number of *cmyb*-expressing HSCs in the CHT (*arrows*), but not in the AGM (*arrowheads*), at 48 hpf **(C, D, G)** and in both the AGM (*arrowheads*) and CHT (*arrows*) at 3 dpf **(E, F, G)** of *Ddx46*$^{hi2137/hi2137}$ larvae was significantly reduced compared with that of *Ddx46*$^{hi2137/+}$ larvae. *Ddx46*$^{hi2137/+}$ larvae: $n=13/13$ (36 hpf), $n=18/18$ (48 hpf), $n=13/13$ (3 dpf); *Ddx46*$^{hi2137/hi2137}$ larvae: $n=9/9$ (36 hpf), $n=14/14$ (48 hpf), $n=11/11$ (3 dpf). *Black dotted lines* in **(C–F)** indicate the boundary between the AGM and CHT. Error bars represent the standard error. *$P<0.01$ by the Student's *t*-test. Scale bars represent 100 μm. Color images available online at www.liebertpub.com/scd

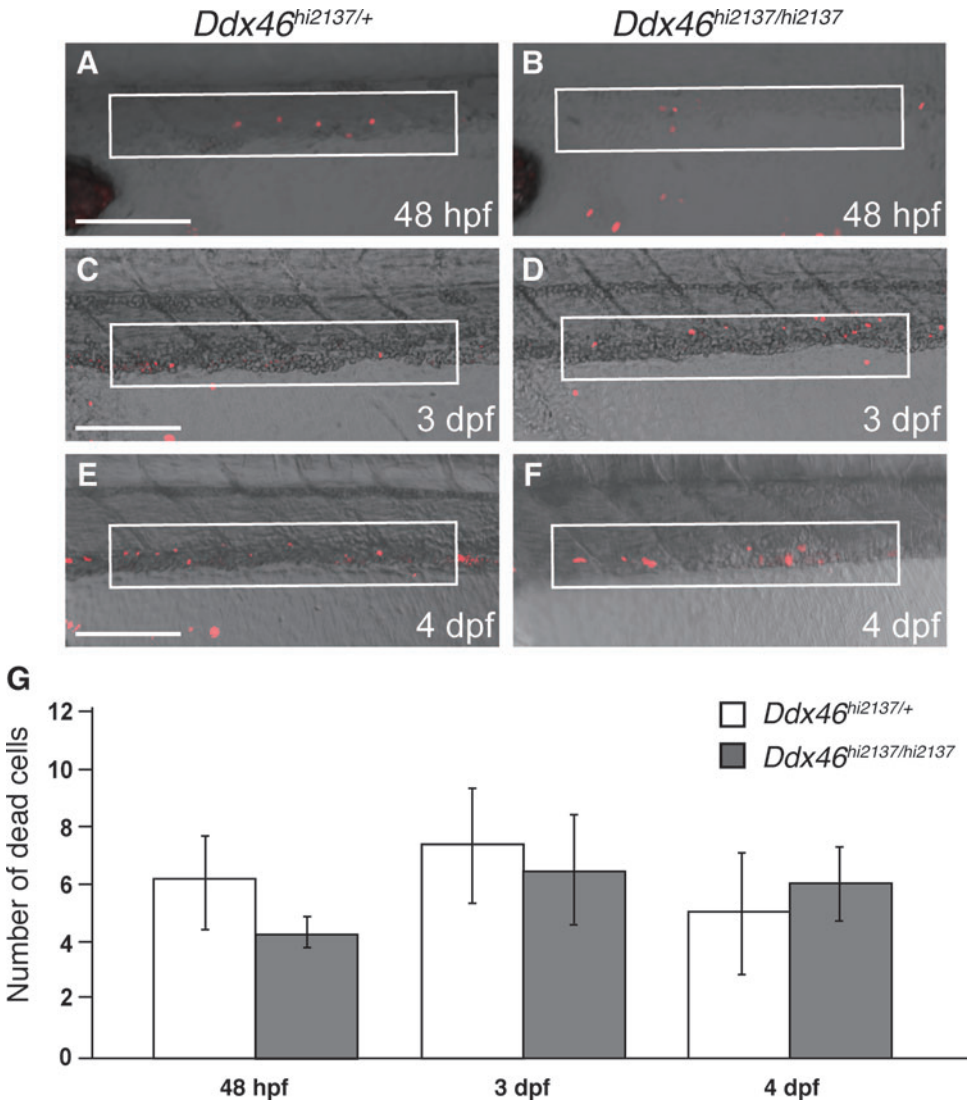

FIG. 5. Cell death is not upregulated in the CHT of *Ddx46*$^{hi2137/hi2137}$ mutants. **(A–F)** Confocal microscopic images of dead cells (*red*) detected by the TUNEL method at 48 hpf, 3 dpf, or 4 dpf. All are lateral views, anterior to the *left*. The *white, boxed regions* show an area of the CHT. **(G)** The number of labeled cells in the *white, boxed regions* **(A–F)** was counted. The number of dead cells in the CHT was indistinguishable between *Ddx46*$^{hi2137/+}$ and *Ddx46*$^{hi2137/hi2137}$ larvae at 48 hpf, 3 dpf, and 4 dpf. *Ddx46*$^{hi2137/+}$ larvae: $n=7/7$ (48 hpf), $n=5/5$ (3 dpf), $n=5/5$ (4 dpf); *Ddx46*$^{hi2137/hi2137}$ larvae: $n=5/5$ (48 hpf), $n=6/6$ (3 dpf), $n=8/8$ (4 dpf). Error bars represent the standard error. Scale bars represent 75 μm. Color images available online at www.liebertpub.com/scd

plastin 1 (*lcp1*) [37] and *mpx*. In contrast to the erythroid and lymphoid markers, myeloid markers were not reduced in *Ddx46*$^{hi2137/hi2137}$ mutants at 3 dpf (Fig. 7I–L). To exclude the possibility that the reduction of erythroid and lymphoid markers was not caused by the deficiency of *Ddx46*, we examined the results of the rescue experiments. We found that *hbae1* and *ikzf1* expression was partially rescued by *Ddx46* mRNA overexpression (Supplementary Fig. S4 and data not shown). Together, these results suggest that HSCs have defects in multilineage differentiation in *Ddx46*$^{hi2137/hi2137}$ mutants: they were able to differentiate to the myeloid fate, but differentiation to the erythroid or lymphoid fate was suppressed in the mutants.

Reduction of gata1a expression leads to erythropoiesis defects in Ddx46$^{hi2137/hi2137}$ *mutants*

Because recent articles have reported that the cross-antagonistic interactions between Gata1a and Spi1 transcription factors are critical for deciding the differentiation to the erythroid or myeloid fate [2,4,5,38], we examined the expression of these genes in *Ddx46*$^{hi2137/hi2137}$ mutants at 3 dpf (Fig. 8A–E). Analyses of in situ hybridization and qPCR revealed that although *gata1a* expression was significantly reduced, *spi1* expression was maintained in the mutants (Fig. 8A–E). To test whether the deficiency of erythropoiesis was caused by the reduction of *gata1a* in *Ddx46*$^{hi2137/hi2137}$ mutants, we carried out rescue experiments. Because phenotypic rescue of vlad tepes (*vlt*), a zebrafish *gata1a* mutant, was not achieved by overexpression of *gata1a* mRNA [39], we tried to use an efficient transient rescue method using the *Tol2* transposable element [29]. We found that the expression of an erythroid marker, *hbae1*, was partially rescued by this *Tol2*-mediated transgenesis method at 3 dpf (Supplementary Fig. S5). These results suggest that the suppression of erythropoiesis in *Ddx46*$^{hi2137/hi2137}$ mutants was due to the reduction of *gata1a* expression.

Ddx46$^{hi2137/hi2137}$ *mutants have defects in pre-mRNA splicing in the hematopoietic cells*

We have previously reported that pre-mRNA splicing of specific genes is defective in *Ddx46*$^{hi2137/hi2137}$ mutants [20]; hence, we examined the pre-mRNA splicing of *gata1a* and

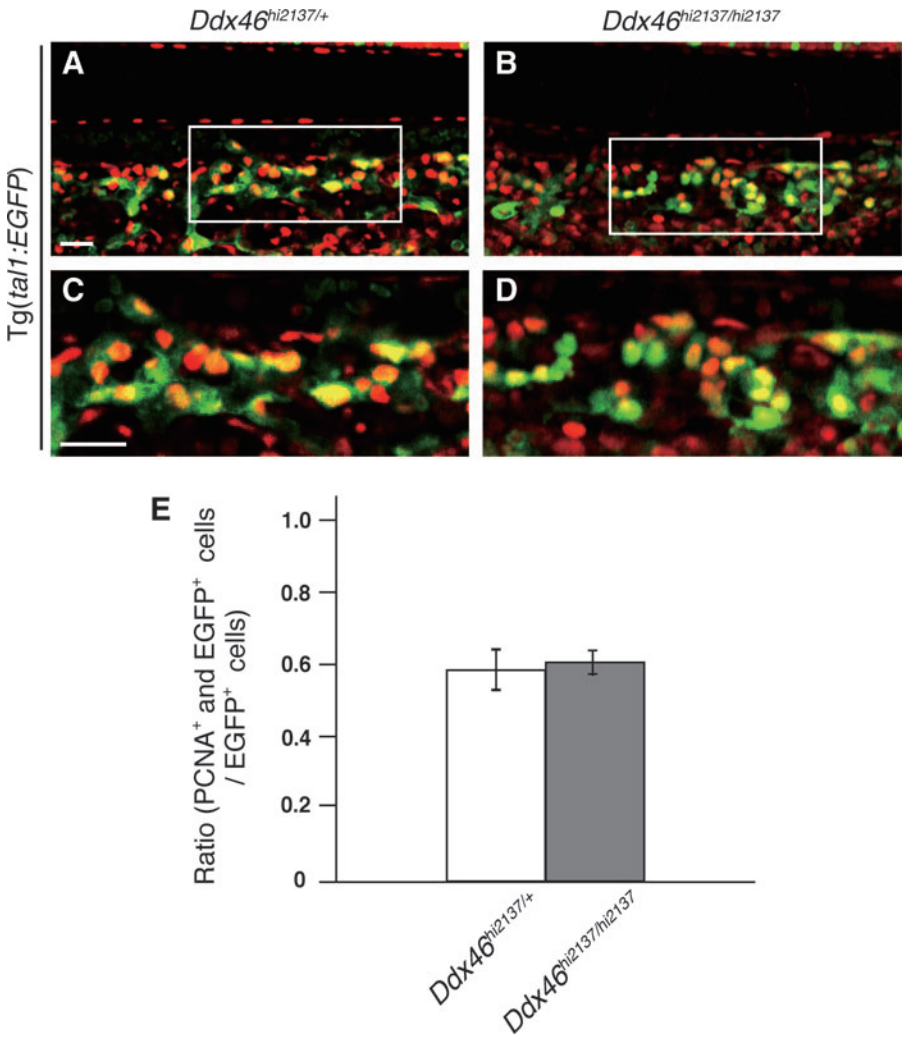

FIG. 6. Cell proliferation is not downregulated in the CHT of *Ddx46*$^{hi2137/hi2137}$ mutants at 48 hpf. **(A–D)** Confocal microscopic images of EGFP fluorescence (*green*) and anti-PCNA (*red*) whole-mount immunostaining of the CHT in *Ddx46*$^{hi2137/+}$;Tg(*tal1:EGFP*) and *Ddx46*$^{hi2137/hi2137}$;Tg(*tal1:EGFP*) larvae at 48 hpf. All are lateral views, anterior to the *left*. Merged single-slice images of cells expressing EGFP (HSCs) and PCNA (proliferating cells). The *boxed areas* in **(A)** and **(B)** are shown enlarged in **(C)** and **(D)**, respectively. **(E)** Quantification of the experiments in panels **(C)** and **(D)** was performed by plotting the ratio of EGFP$^+$ and PCNA$^+$ cells (*yellow*) to the total number of EGFP$^+$ cells (*green* and *yellow*). No significant difference between *Ddx46*$^{hi2137/+}$;Tg(*tal1:EGFP*) and *Ddx46*$^{hi2137/hi2137}$;Tg(*tal1:EGFP*) larvae was observed. Cells were counted from four single slices from four embryos for each condition. Error bars represent the standard error. The scale bar represents 20 μm. PCNA, proliferating cell nuclear antigen. Color images available online at www.liebertpub.com/scd

spi1 by RT-PCR in this study. The RT-PCR analyses showed that although the unspliced mRNAs of *gata1a* were retained, the pre-mRNA splicing of *spi1* was normal in *Ddx46*$^{hi2137/hi2137}$ mutants at 3 dpf (Fig. 8F–I). It is possible that the defects in pre-mRNA splicing lead to the reduction of *gata1a* expression and suppression of erythropoiesis in *Ddx46*$^{hi2137/hi2137}$ mutants. In addition to *gata1a* and *spi1*, we tested the pre-mRNA splicing of *cmyb* to examine the effect in HSCs. Similarly to *gata1a*, the unspliced mRNAs of *cmyb* were retained in *Ddx46*$^{hi2137/hi2137}$ mutants at 3 dpf (Fig. 8J, K), suggesting that the defects in pre-mRNA splicing may affect the multilineage differentiation of HSCs.

Discussion

Status of HSCs in Ddx46$^{hi2137/hi2137}$ *mutants*

Although the expression of molecular markers for HSCs, such as *tal1*, *runx1*, or *cmyb*, was markedly reduced and proliferation of the HSCs was normal at 48 hpf, massive cell death of HSCs was not detected in *Ddx46*$^{hi2137/hi2137}$ mutants. There are several possibilities to explain the status of HSCs in *Ddx46*$^{hi2137/hi2137}$ mutants. One possible explanation is that, although the differentiation of HSCs is restricted to myeloid fate at the beginning of definitive hematopoiesis (around 30 hpf), the ability of differentiation to myeloid fate is lost at later stages, probably due to the reduction of *tal1*, *runx1*, and *cmyb* expressions in *Ddx46*$^{hi2137/hi2137}$ mutants at 3 dpf. Since previous studies have reported that Cmyb could regulate the expression of *tal1* and *runx1* in zebrafish and mouse HSCs, respectively [9,40], it is possible that splicing defects in *cmyb* result in the reduction of *tal1* and *runx1* expressions in HSCs of *Ddx46*$^{hi2137/hi2137}$ mutants. Another possibility is that HSCs continue to produce myeloid cells without the expressions of *tal1*, *runx1*, and *cmyb* during definitive hematopoiesis in *Ddx46*$^{hi2137/hi2137}$ mutants. Alternative possibility is that HSCs are lost, and they prematurely differentiate into myeloid cells. In both scenarios, the number of *lcp1*- or *mpx*-expressing myeloid cells should be increased in the mutants throughout definitive hematopoiesis. Since we have not analyzed the expression of molecular markers for myeloid cells at the beginning of definitive hematopoiesis, it is interesting to examine *spi1* expression in *Ddx46*$^{hi2137/hi2137}$ mutants at around 30 hpf. However, we showed that there was no striking difference in the number of myeloid cells between *Ddx46*$^{hi2137/+}$ and *Ddx46*$^{hi2137/hi2137}$ larvae at 3 dpf (Fig. 7). Therefore, it is possible that the proliferation of the HSCs is reduced after 2.5 dpf. Unfortunately, due to the

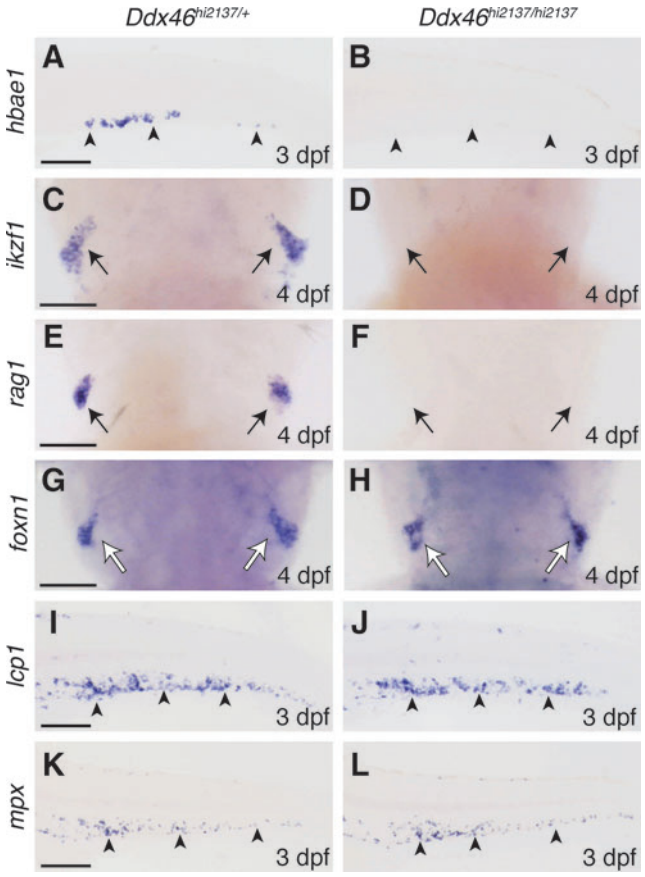

FIG. 7. Myelopoiesis occurs, but erythropoiesis and lymphopoiesis are suppressed in *Ddx46*$^{hi2137/hi2137}$ mutants. **(A–L)** The expression of molecular markers for erythrocytes, lymphocytes, myelocytes, and a thymus epithelium was examined by whole-mount in situ hybridization at 3 and 4 dpf. Lateral views, anterior to the *left* **(A, B, I–L)**. Dorsal views, anterior to the *top* **(C–H)**. The expression of a definitive erythroid marker *hbae1* was markedly reduced in *Ddx46*$^{hi2137/hi2137}$ larvae at 3 dpf **(***arrowheads* in **A, B)** (*Ddx46*$^{hi2137/hi2137}$ larvae, $n=7/7$; *Ddx46*$^{hi2137/+}$ larvae, $n=9/9$). The expression of lymphoid markers, *ikzf1* (*Ddx46*$^{hi2137/hi2137}$ larvae, $n=9/9$; *Ddx46*$^{hi2137/+}$ larvae, $n=9/9$) and *rag1* (*Ddx46*$^{hi2137/hi2137}$ larvae, $n=9/9$; *Ddx46*$^{hi2137/+}$ larvae, $n=7/7$), was lost in *Ddx46*$^{hi2137/hi2137}$ larvae **(***black arrows* in **C–F)**, whereas the expression of a thymus epithelial marker *foxn1* was indistinguishable between *Ddx46*$^{hi2137/+}$ ($n=7/7$) and *Ddx46*$^{hi2137/hi2137}$ larvae ($n=9/9$) at 4 dpf **(***white arrows* in **G, H)**. In contrast, the expression of myeloid markers, *lcp1* (*Ddx46*$^{hi2137/hi2137}$ larvae, $n=8/8$; *Ddx46*$^{hi2137/+}$ larvae, $n=8/8$) and *mpx* (*Ddx46*$^{hi2137/hi2137}$ larvae, $n=12/13$; *Ddx46*$^{hi2137/+}$ larvae, $n=8/8$), was maintained in *Ddx46*$^{hi2137/hi2137}$ larvae at 3 dpf **(***arrowheads* in **I–L)**. Scale bars represent 100 μm. *hbae1*, hemoglobin alpha embryonic-1; *ikzf1*, IKAROS family zinc finger 1; *rag1*, recombination activating gene 1; *foxn1*, forkhead box N1; *lcp1*, lymphocyte cytosolic plastin 1. Color images available online at www.liebertpub.com/scd

downregulation of EGFP fluorescence at 3 dpf, it was very difficult to evaluate the proliferation of HSCs using the Tg(*tal1:EGFP*) line (Supplementary Fig. S3). In contrast to *tal1*, the number of *cmyb*-expressing cells is higher than that of *tal1*-expressing cells during definitive hematopoiesis; this finding could be related to the fact that mouse *cmyb* is expressed in HSCs and progenitor cells [5]. In addition, *cmyb*-expressing cells are still present in *Ddx46*$^{hi2137/hi2137}$ mutants at 3 dpf (Fig. 4G). Therefore, it may be important to analyze the cell proliferation after 2.5 dpf by using the *cmyb:EGFP* transgenic line. Currently, the presence of HSCs in *Ddx46*$^{hi2137/hi2137}$ mutants remains unknown because molecular markers of HSCs for maintenance and differentiation, except *tal1*, *runx1*, and *cmyb*, have not yet been reported in zebrafish. Further studies will therefore be necessary to identify the key target genes affected by the loss of Ddx46 function for the maintenance and differentiation of HSCs.

Role of pre-mRNA splicing factors in hematopoiesis

Because pre-mRNA splicing of *gata1a* and *cmyb*, but not *spi1*, is defective in *Ddx46*$^{hi2137/hi2137}$ mutants (Fig. 8), it is possible that aberrant pre-mRNAs lead to reduced *gata1a* and *cmyb* expressions. Our results suggest that pre-mRNA splicing is associated with hematopoiesis in zebrafish. Recently, numerous studies using whole-exome sequencing revealed that recurrent mutations in spliceosome subunits have been implicated in hematopoietic malignancies [41–44]. The 4 genes encoding spliceosome components, U2 small nuclear RNA auxiliary factor 1 (*U2AF1*; also known as *U2AF35*), splicing factor 3B subunit 1 (*SF3B1*), U2AF1-related protein (*ZRSR2*; also known as *Urp*), and serine/arginine-rich splicing factor 2 (*SRSF2*), are frequently mutated in chronic lymphocytic leukemia (CLL) and/or myelodysplastic syndrome (MDS) [41–44]. It is well known that these 4 components are involved in the initial steps of pre-mRNA splicing for the establishment of spliceosome complexes E and A: U2AF1 and SRSF2 bind to the 3′ splice acceptor site of the pre-mRNA: ZRSR2 interacts with U2AF1 and a serine/arginine-rich SR protein: and SF3B1, which is a component of the U2 small nuclear ribonucleoprotein (U2snRNP), binds to the branch point sequence of the pre-mRNA [45,46]. These results suggest that the initial steps of pre-mRNA splicing are closely related to hematopoietic malignancies in mammals.

Yeast DExD/H-box proteins, Sub2, Prp5, Prp28, Brr2, Prp2, Prp16, Prp22, and Prp43, act in specific steps of the splicing cycles to catalyze RNA–RNA rearrangements and RNP remodeling [16,17]. Among these, it has been determined that *Saccharomyces cerevisiae* Prp5 (a yeast orthologue of vertebrate Ddx46) and human DDX46 are able to interact with U2snRNP [16,17,47]. These reports, combined with the splicing factor studies in hematopoietic malignancies, suggest that the 4 splicing components (U2AF1, SF3B1, ZRSR2, and SRSF2) and Ddx46 play critical roles in the initial steps of pre-mRNA splicing, and these factors may function in the maintenance and/or differentiation of HSCs. Although recurrent mutations in DDX46 have not yet been reported in patients with CLL and/or MDS by whole-exome sequencing, it is possible that mutations in DDX46 cause hematopoietic malignancies.

Control of hematopoiesis by DExD/H-box RNA helicases

A recent report has revealed that Dhx8, a zebrafish orthologue of the yeast splicing factor Prp22, is involved in pre-mRNA splicing and is required for primitive hematopoiesis [19]. In contrast to Prp5/Ddx46, the function of yeast Prp22 is critical for spliceosome disassembly when splicing

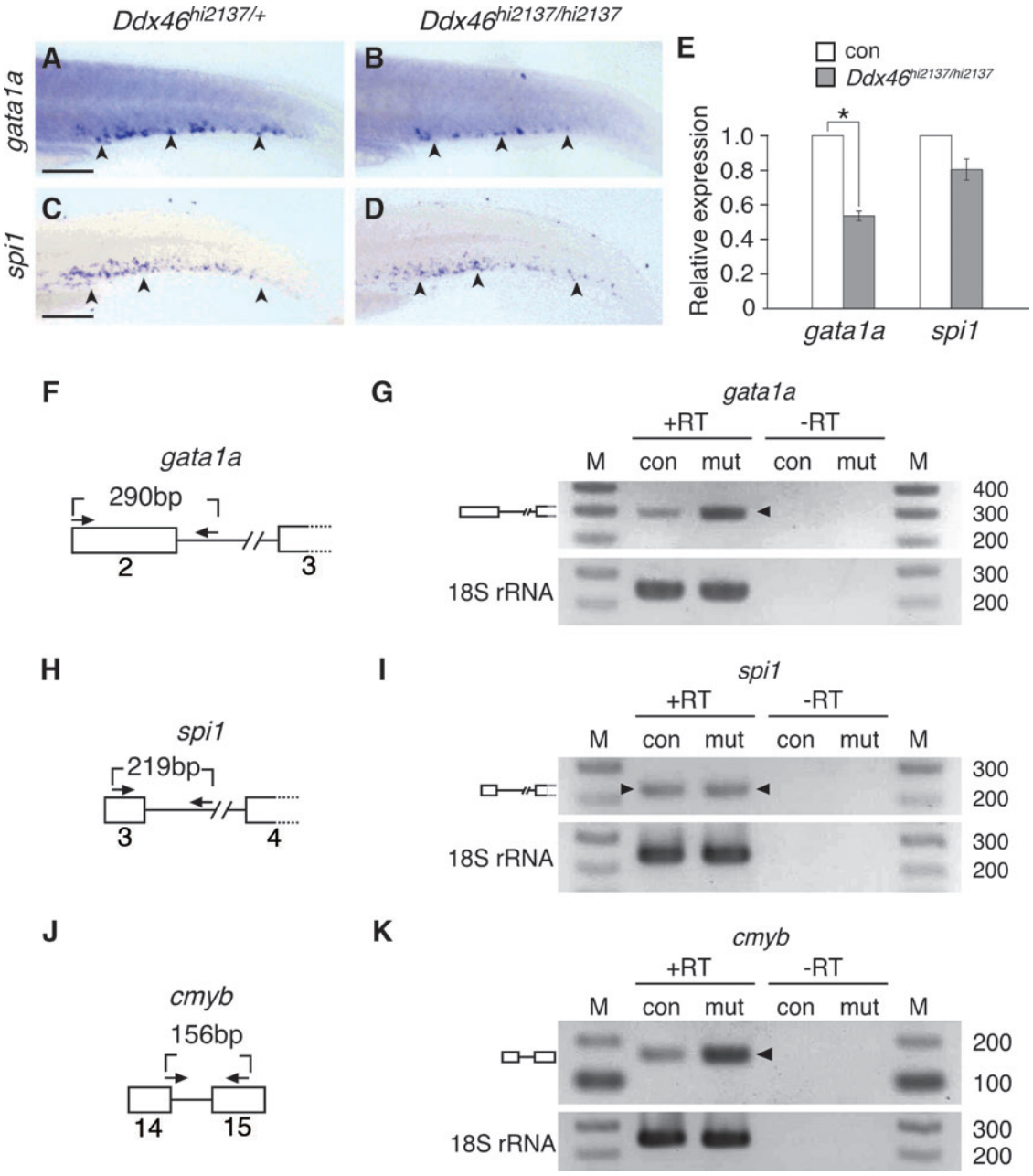

FIG. 8. Expression and pre-mRNA splicing of *gata1a*, but not *spi1*, are defective in *Ddx46*$^{hi2137/hi2137}$ mutants. **(A–D)** The expression of *gata1a* and *spi1* was examined by whole-mount in situ hybridization at 3 dpf. All are lateral views, anterior to the *left*. The expression of *gata1a* in the CHT of *Ddx46*$^{hi2137/hi2137}$ larvae ($n = 10/10$) was markedly reduced compared with that of *Ddx46*$^{hi2137/+}$ larvae ($n = 10/10$) **(***arrowheads* in **A, B)**. In contrast, *spi1* expression in the CHT of *Ddx46*$^{hi2137/hi2137}$ larvae ($n = 10/10$) was maintained compared with that of *Ddx46*$^{hi2137/+}$ larvae ($n = 9/9$) **(***arrowheads* in **C, D)**. Scale bars represent 100 μm. **(E)** Relative expression of *gata1a* and *spi1* genes in control (con) larvae compared with that in *Ddx46*$^{hi2137/hi2137}$ larvae at 3 dpf, by qPCR. Although no significant difference of *spi1* expression was found between con and *Ddx46*$^{hi2137/hi2137}$ larvae, *gata1a* expression in *Ddx46*$^{hi2137/hi2137}$ larvae was significantly lower than that in con larvae. *$P < 0.01$ by the Student's *t*-test. Error bars represent the standard error. **(F–K)** Schematic drawings of the *gata1a*, *spi1*, and *cmyb* pre-mRNA regions analyzed for splicing (*boxes*, exons; *lines*, introns; *arrows*, primers) **(F, H, J)**. The splicing status of *gata1a*, *spi1*, or *cmyb* pre-mRNA was monitored by RT-PCR with the primers indicated in schemes **(F)**, **(H)**, or **(J)**, respectively. The reverse primer for *gata1a* or *spi1* mRNA was designed within the intron **(F, H)**. The forward primer for *cmyb* crosses the exon14/intron14 boundary **(J)**. Unspliced *gata1a* or *cmyb* mRNA was retained at a higher level in *Ddx46*$^{hi2137/hi2137}$ mutant (mut) larvae than in con larvae **(***arrowhead* in **G** = 290 bp; *arrowhead* in **K** = 156 bp**)**. In contrast, the level of unspliced *spi1* mRNA was indistinguishable between the mut larvae and con larvae **(***arrowheads* in **I** = 219 bp**)**. Unspliced PCR products were verified by sequencing. +RT refers to the validation reaction itself, and −RT represents the respective control reaction without reverse transcriptase. 18S rRNA is a loading control. Control larvae were sibling WT or *Ddx46*$^{hi2137/+}$ larvae, and they had normal phenotypes. qPCR, quantitative polymerase chain reaction; RT, reverse transcription. Color images available online at www.liebertpub.com/scd

reactions have been completed [16,17]. Although both *Ddx46* and *Dhx8* are maternal genes and are ubiquitously expressed during early somitogenesis, *Dhx8* mutants, but not *Ddx46*$^{hi2137/hi2137}$ mutants, showed defects in primitive hematopoiesis. One possible explanation for this phenotypic difference between *Ddx46*$^{hi2137/hi2137}$ and *Dhx8* mutants is that the function of Ddx46 is not necessary for primitive hematopoiesis and is specific for the control of HSC differentiation in zebrafish larvae. Alternatively, it is possible that because maternal transcripts of *Ddx46* or maternally derived Ddx46 proteins are more stable than those of Dhx8, defects in primitive hematopoiesis are rescued in *Ddx46*$^{hi2137/hi2137}$ mutants. Further studies will be needed to elucidate the detailed mechanisms that lead to hematopoiesis deficiencies and related diseases that are caused by DExD/H-box RNA helicases and/or splicing factors.

Acknowledgements

We thank the members of Kikuchi and Atsushi Suzuki laboratories in Hiroshima University for helpful discussion and critical comments. We also thank Drs. Atsuo Kawahara and Makoto Kobayashi for providing DNA templates. This work was supported by a grant from the Sasakawa Foundation to R.H., The Sasakawa Foundation and the Kao Foundation for Arts and Sciences to S.H., and grant-in-aid for Scientific Research from the JSPS (KAKENHI 15370094 and 19570204) to Y.K.

Author Disclosure Statement

There are no conflicts of interest in this article.

References

1. Cumano A and I Godin. (2007). Ontogeny of the hematopoietic system. Annu Rev Immunol 25:745–785.
2. Orkin SH and LI Zon. (2008). Hematopoiesis: an evolving paradigm for stem cell biology. Cell 132:631–644.
3. Medvinsky A, S Rybtsov and S Taoudi. (2011). Embryonic origin of the adult hematopoietic system: advances and questions. Development 138:1017–1031.
4. Carradice D and GJ Lieschke. (2008). Zebrafish in hematology: sushi or science? Blood 111:3331–3342.
5. Paik EJ and LI Zon. (2010). Hematopoietic development in the zebrafish. Int J Dev Biol 54:1127–1137.
6. Mucenski ML, K McLain, AB Kier, SH Swerdlow, CM Schreiner, TA Miller, DW Pietryga, WJ Scott and SS Potter. (1991). A functional c-myb gene is required for normal murine fetal hepatic hematopoiesis. Cell 65:677–689.
7. Sumner R, A Crawford, M Mucenski and J Frampton. (2000). Initiation of adult myelopoiesis can occur in the absence of c-Myb whereas subsequent development is strictly dependent on the transcription factor. Oncogene 19:3335–3342.
8. Lieu YK and EP Reddy. (2009). Conditional c-myb knockout in adult hematopoietic stem cells leads to loss of self-renewal due to impaired proliferation and accelerated differentiation. Proc Natl Acad Sci U S A 106:21689–21694.
9. Soza-Ried C, I Hess, N Netuschil, M Schorpp and T Boehm. (2010). Essential role of c-myb in definitive hematopoiesis is evolutionarily conserved. Proc Natl Acad Sci U S A 107:17304–17308.
10. Zhang Y, H Jin, L Li, FX Qin and Z Wen. (2011). cMyb regulates hematopoietic stem/progenitor cell mobilization during zebrafish hematopoiesis. Blood 118:4093–4101.
11. North TE, MF de Bruijn, T Stacy, L Talebian, E Lind, C Robin, M Binder, E Dzierzak and NA Speck. (2002). Runx1 expression marks long-term repopulating hematopoietic stem cells in the midgestation mouse embryo. Immunity 16:661–672.
12. Burns CE, T DeBlasio, Y Zhou, J Zhang, L Zon and SD Nimer. (2002). Isolation and characterization of runxa and runxb, zebrafish members of the runt family of transcriptional regulators. Exp Hematol 30:1381–1389.
13. Chen MJ, T Yokomizo, BM Zeigler, E Dzierzak and NA Speck. (2009). Runx1 is required for the endothelial to haematopoietic cell transition but not thereafter. Nature 457: 887–891.
14. Sood R, MA English, CL Belele, H Jin, K Bishop, R Haskins, MC McKinney, J Chahal, BM Weinstein, Z Wen and PP Liu. (2010). Development of multilineage adult hematopoiesis in the zebrafish with a runx1 truncation mutation. Blood 115: 2806–2809.
15. Lancrin C, P Sroczynska, C Stephenson, T Allen, V Kouskoff and G Lacaud. (2009). The haemangioblast generates haematopoietic cells through a haemogenic endothelium stage. Nature 457:892–895.
16. Rocak S and P Linder. (2004). DEAD-box proteins: the driving forces behind RNA metabolism. Nat Rev Mol Cell Biol 5:232–241.
17. Bleichert F and S Baserga. (2007). The long unwinding road of RNA helicases. Mol Cell 27:339–352.
18. Payne EM, N Bolli, J Rhodes, OI Abdel-Wahab, R Levine, CV Hedvat, R Stone, A Khanna-Gupta, H Sun, et al. (2011). Ddx18 is essential for cell-cycle progression in zebrafish hematopoietic cells and is mutated in human AML. Blood 118:903–915.
19. English MA, L Lei, T Blake, SM Wincovitch, R Sood, M Azuma, D Hickstein and P Paul Liu. (2012). Incomplete splicing, cell division defects and hematopoietic blockage in dhx8 mutant zebrafish. Dev Dyn 241:879–889.
20. Hozumi S, R Hirabayashi, A Yoshizawa, M Ogata, T Ishitani, M Tsutsumi, A Kuroiwa, M Itoh and Y Kikuchi. (2012). DEAD-box protein Ddx46 is required for the development of the digestive organs and brain in zebrafish. PLoS One 7:e33675.
21. Westerfield, M. *The Zebrafish Book: A Guide for the Laboratory Use of Zebrafish* (*Danio rerio*), 4th edn. University of Oregon Press, Eugene, OR, 2000.
22. Kimmel CB, WW Ballard, SR Kimmel, B Ullmann and TF Schilling. (1995). Stages of embryonic development of the zebrafish. Dev Dyn 203:253–310.
23. Amsterdam A, R Nissen, Z Sun, E Swindell, S Farrington and N Hopkins. (2004). Identification of 315 genes essential for early zebrafish development. Proc Natl Acad Sci U S A 101:12792–12797.
24. Gering M, AR Rodaway, B Göttgens, RK Patient and AR Green. (1998). The SCL gene specifies haemangioblast development from early mesoderm. EMBO J 17:4029–4045.
25. Zhang XY and AR Rodaway. (2007). SCL-GFP transgenic zebrafish: *in vivo* imaging of blood and endothelial development and identification of the initial site of definitive hematopoiesis. Dev Biol 307:179–194.
26. Urasaki A, G Morvan and K Kawakami. (2006). Functional dissection of the Tol2 transposable element identified the minimal cis-sequence and a highly repetitive sequence in the

subterminal region essential for transposition. Genetics 174:639–649.
27. Mizoguchi T, H Verkade, JK Heath, A Kuroiwa and Y Kikuchi. (2008). Sdf1/Cxcr4 signaling controls the dorsal migration of endodermal cells during zebrafish gastrulation. Development 135:2521–2529.
28. Detrich HW, MW Kieran, FY Chan, LM Barone, K Yee, JA Rundstadler, S Pratt, D Ransom and LI Zon. (1995). Intraembryonic hematopoietic cell migration during vertebrate development. Proc Natl Acad Sci U S A 92:10713–10717.
29. Takeuchi M, H Kaneko, K Nishikawa, K Kawakami, M Yamamoto and M Kobayashi. (2010). Efficient transient rescue of hematopoietic mutant phenotypes in zebrafish using Tol2-mediated transgenesis. Dev Growth Differ 52: 245–250.
30. Lieschke GJ, AC Oates, BH Paw, MA Thompson, NE Hall, AC Ward, RK Ho, LI Zon and JE Layton. (2002). Zebrafish SPI-1 (PU.1) marks a site of myeloid development independent of primitive erythropoiesis: implications for axial patterning. Dev Biol 246:274–295.
31. Thompson MA, DG Ransom, SJ Pratt, H MacLennan, MW Kieran, HW Detrich, B Vail, TL Huber, B Paw, et al. (1998). The cloche and spadetail genes differentially affect hematopoiesis and vasculogenesis. Dev Biol 197:248–269.
32. Brownlie A, C Hersey, AC Oates, BH Paw, AM Falick, HE Witkowska, J Flint, D Higgs, J Jessen, et al. (2003). Characterization of embryonic globin genes of the zebrafish. Dev Biol 255:48–61.
33. Bennett CM, JP Kanki, J Rhodes, TX Liu, BH Paw, MW Kieran, DM Langenau, A Delahaye-Brown, LI Zon, MD Fleming and AT Look. (2001). Myelopoiesis in the zebrafish, *Danio rerio*. Blood 98:643–651.
34. Willett CE, H Kawasaki, CT Amemiya, S Lin and LA Steiner. (2001). Ikaros expression as a marker for lymphoid progenitors during zebrafish development. Dev Dyn 222: 694–698.
35. Willett CE, AG Zapata, N Hopkins and LA Steiner. (1997). Expression of zebrafish rag genes during early development identifies the thymus. Dev Biol 182:331–341.
36. Schorpp M, M Leicht, E Nold, M Hammerschmidt, A Haas-Assenbaum, W Wiest and T Boehm. (2002). A zebrafish orthologue (whnb) of the mouse nude gene is expressed in the epithelial compartment of the embryonic thymic rudiment. Mech Dev 118:179–185.
37. Herbomel P, B Thisse and C Thisse. (1999). Ontogeny and behaviour of early macrophages in the zebrafish embryo. Development 126:3735–3745.
38. Monteiro R, C Pouget and R Patient. (2011). The gata1/pu.1 lineage fate paradigm varies between blood populations and is modulated by tif1γ. EMBO J 30:1093–1103.
39. Lyons SE, ND Lawson, L Lei, PE Bennett, BM Weinstein and PP Liu. (2002). A nonsense mutation in zebrafish gata1 causes the bloodless phenotype in vlad tepes. Proc Natl Acad Sci U S A 99:5454–5459.
40. Dai G, H Sakamoto, Y Shimoda, T Fujimoto, S Nishikawa and M Ogawa. (2006). Over-expression of c-Myb increases the frequency of hemogenic precursors in the endothelial cell population. Genes Cells 11:859–870.
41. Yoshida K, M Sanada, Y Shiraishi, D Nowak, Y Nagata, R Yamamoto, Y Sato, A Sato-Otsubo, A Kon, et al. (2011). Frequent pathway mutations of splicing machinery in myelodysplasia. Nature 478:64–69.
42. Hahn CN and HS Scott. (2012). Spliceosome mutations in hematopoietic malignancies. Nat Genet 44:9–10.
43. Quesada V, L Conde, N Villamor, GR Ordóñez, P Jares, L Bassaganyas, AJ Ramsay, S Beà, M Pinyol, et al. (2012). Exome sequencing identifies recurrent mutations of the splicing factor SF3B1 gene in chronic lymphocytic leukemia. Nat Genet 44:47–52.
44. Graubert TA, D Shen, L Ding, T Okeyo-Owuor, CL Lunn, J Shao, K Krysiak, CC Harris, DC Koboldt, et al. (2012). Recurrent mutations in the U2AF1 splicing factor in myelodysplastic syndromes. Nat Genet 44:53–57.
45. Tronchère H, J Wang and XD Fu. (1997). A protein related to splicing factor U2AF35 that interacts with U2AF65 and SR proteins in splicing of pre-mRNA. Nature 388:397–400.
46. Wahl MC, CL Will and R Lührmann. (2009). The spliceosome: design principles of a dynamic RNP machine. Cell 136:701–718.
47. Xu YZ, CM Newnham, S Kameoka, T Huang, MM Konarska and CC Query. (2004). Prp5 bridges U1 and U2 snRNPs and enables stable U2 snRNP association with intron RNA. EMBO J 23:376–385.

Address correspondence to:
Dr. Yutaka Kikuchi
Department of Biological Science
Graduate School of Science
Hiroshima University
Kagamiyama 1-3-1
Higashi-Hiroshima
Hiroshima 739-8526
Japan

E-mail: yutaka@hiroshima-u.ac.jp

Received for publication November 6, 2012
Accepted after revision April 30, 2013
Prepublished on Liebert Instant Online May 1, 2013